energies

MDPI

Article

Short-Term Solar Power Predicting Model Based on Multi-Step CNN Stacked LSTM Technique

Neethu Elizabeth Michael [1], Manohar Mishra [2], Shazia Hasan [1,*] and Ahmed Al-Durra [3]

[1] Department of Electrical and Electronics Engineering, Birla Institute of Technology and Science Pilani, Dubai Campus, Dubai P.O. Box 345055, United Arab Emirates; p20180008@dubai.bits-pilani.ac.in
[2] Department of Electrical and Electronics Engineering, Institute of Technical Education and Research, Siksha 'O' Anusandhan University, Bhubaneswar P.O. Box 751030, India; manoharmishra@soauniversity.ac.in
[3] Department of Electrical and Computer Engineering, Khalifa University, Abu Dhabi P.O. Box 127788, United Arab Emirates; ahmed.aldurra@ku.ac.ae
* Correspondence: dr.shaziahasan@gmail.com

Abstract: Variability in solar irradiance has an impact on the stability of solar systems and the grid's safety. With the decreasing cost of solar panels and recent advancements in energy conversion technology, precise solar energy forecasting is critical for energy system integration. Despite extensive research, there is still potential for advancement of solar irradiance prediction accuracy, especially global horizontal irradiance. Global Horizontal Irradiance (GHI) (unit: KWh/m^2) and the Plane Of Array (POA) irradiance (unit: W/m^2) were used as the forecasting objectives in this research, and a hybrid short-term solar irradiance prediction model called modified multi-step Convolutional Neural Network (CNN)-stacked Long-Short-Term-Memory network (LSTM) with drop-out was proposed. The real solar data from Sweihan Photovoltaic Independent Power Project in Abu Dhabi, UAE is preprocessed, and features were extracted using modified CNN layers. The output result from CNN is used to predict the targets using a stacked LSTM network and the efficiency is proved by comparing statistical performance measures in terms of Root Mean Square Error (*RMSE*), Mean Absolute Percentage Error (*MAPE*), Mean Squared Error (*MAE*), and R^2 scores, with other contemporary machine learning and deep-learning-based models. The proposed model offered the best *RMSE* and R^2 values of 0.36 and 0.98 for solar irradiance prediction and 61.24 with R^2 0.96 for POA prediction, which also showed better performance as compared to the published works in the literature.

Keywords: convolution neural network; deep learning; plane of array (POA) irradiance; solar Irradiance; solar forecasting; stacked LSTM

Citation: Elizabeth Michael, N.; Mishra, M.; Hasan, S.; Al-Durra, A. Short-Term Solar Power Predicting Model Based on Multi-Step CNN Stacked LSTM Technique. *Energies* **2022**, *15*, 2150. https://doi.org/10.3390/en15062150

Academic Editors: Pedro Dinis Gaspar, Pedro Dinho da Silva and Luís C. Pires

Received: 9 February 2022
Accepted: 8 March 2022
Published: 15 March 2022

1. Introduction

Global energy requirements have been gradually growing for the past several decades. On the other hand, the availability of fossil fuel resources is also a question mark as the consumption rate is growing speedily. Among RES, Solar Photo Voltaic (SPV) energy, as one of the potential alternatives for fossil fuel-based energy generation, has been a significant solution in recent times owing to the benefits of being copious, infinite, and cleanse [1]. Figure 1 shows the rate of new capacity additions worldwide, where the dominancy in PV installation can be observed. According to the recent study reported in [2], the installed power capacity of global PV systems has expanded dramatically from 39 GW in 2010 to 760 GW in 2020. Figure 1 also shows the rate of installed SPV power capacity installed in the last decade. Moreover, it is expected that the rate of SPV integrations to the main grid will be increased further because of decreased SPV module prices and the increased rate of depletion rate of fossil fuels.

However, owing to the untidy and unpredictable characteristics of the climate conditions, the power production from the SPV system always exposes solid insecurities through intermittency, volatility, and uncertainty [3]. These ambiguities may damage

the instantaneous control performance, diminish system economics, and hence stress the electrical power and utility system [4]. In this regard, it is important to suggest a precise SPV power prediction model concerning system dependability, reliability, and power dispatching ability.

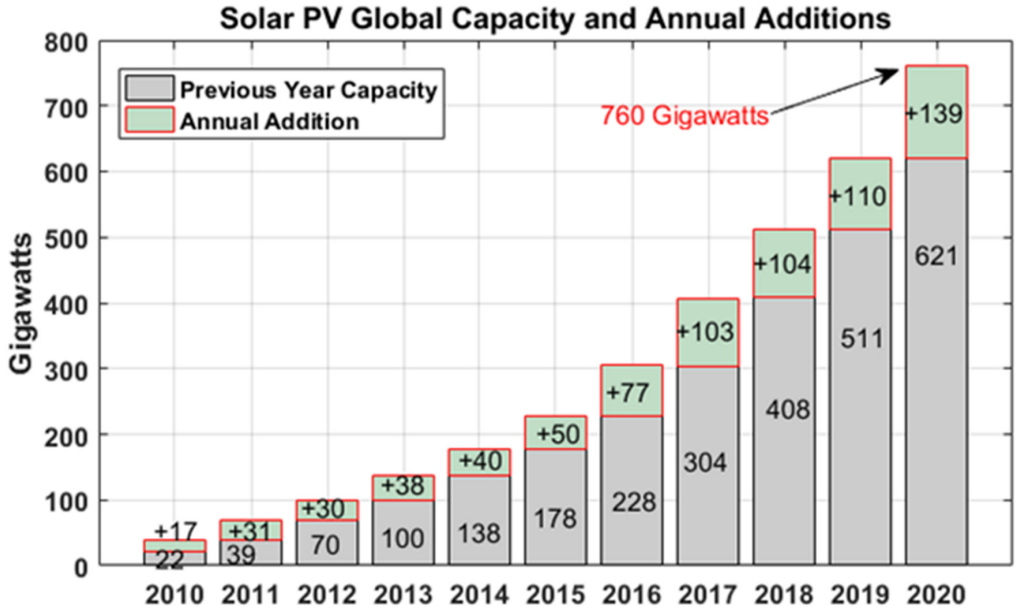

Figure 1. Status of renewable sources installations worldwide.

In recent times, several SPV output power prediction models have been proposed for different time horizons (such as short-term, medium-term, and long-term). These methods can be categorized into two groups according to the principle of operation: indirect and direct methods [4]. In the earlier method, one is to forecast the SPV panel temperature, solar irradiance, and additional factors allied with SPV power production. Afterward, the predicted upshots are fed as input to the SPV prediction model to achieve the SPV output power [5]. On the other hand, the prior method is based on several historical time-series data, including output power, atmospheric temperature, solar radiation, cloud coverage, and wind speed [5]. The indirect approach has a very complex architecture with lower prediction accuracy. On the other hand, the direct approach has been studied and applied widely. In addition to this classification, the PV power forecasting approaches are again classified into persistence model, statistical model, and Machine Learning (ML) model-based methods [6]. Unfortunately, the first two approaches show comparatively low forecasting accuracy and are also ineffective to deal with the non-linear relationship between several meteorological data and solar irradiance [5]. Moreover, considering the high computational cost involved in the persistence model-based approach [7] and the necessities of error minimization algorithm in statistical model-based approach [8]; the ML-based approach has got huge attention in the last decades [9,10]. In the ML model framework, several techniques have already been implemented for accurate prediction of PV power, such as Support Vector Machine (SVM), Artificial Neural Network (ANN), Extreme Learning Machine (ELM), and metaheuristic techniques.

Although the ML algorithm has several advantages like fast, reasonable, and simple architecture, Deep Learning (DL) uses a complex structure of the neural network to learn the data and pattern [11]. DL can allow extremely noisy datasets and incorporate irrelevant datasets, and likewise elucidate non-linear correlations in the dataset [11]. Additionally, it can also learn the features without additional feature engineering. In the last couple of years, the applications of DL-based approaches have gained huge attention in time-series prediction. In this regard, a few DL approaches have been reported to predict solar power in the literature, such as LSTM [12], Recurrent Neural Network (RNN) [13], CNN [14],

Autoencoder [15], Deep Convolutional Neural Network (DCNN) [16], Deep Belief Network (DBN) [17], etc. In each of these methods, the superiority of DL over ML approaches has been clearly explained. A three-dimensional Convolutional Neural Network (3D-CNN) is created by Zhao et al. [18] to achieve historical information and then fed the data features into a Multi-Layer Perceptron (MLP). Unfortunately, since the nodes between the hidden layers are not connected, an MLP cannot preserve the long-term memory of an input time series. Since the LSTM has a complex memory unit to remember the previous information, it gives better performance accuracy with time-series data. However, the existing solar irradiance prediction methods based on CNN have accuracy limits that cannot be ignored. Some extended literature surveys can be found in Table 1. This table shows a bibliographic analysis using DL for solar forecasting.

Hence, to increase the accuracy of the prediction model, hybridization of these DL models was also successfully carried out by different researchers for different applications, for example, CNN-LSTM [19] (short-term load forecasting model), LSTM-RNN [20] (short-term solar forecasting), etc. The output results corresponding to these hybrid models shows an incremental accuracy level compared to solo techniques. Considering the advantages of DL hybrid models and overcoming the shortcomings of the above-mentioned models, the objectives of this work are:

a. To apply novel hybrid solar power prediction model named 'multi-step CNN-stacked LSTM with drop-out deep learning method for improved effectiveness as compared to other traditional methods of solar irradiance forecasting.
b. To forecast a highly accurate solar irradiance that would help mitigate the challenges posed by the stochastic nature of solar energy production to power grid operations.
c. To use real-world solar data that is taken from Sweihan Photovoltaic Independent Power Project, Abu Dhabi.

Table 1. Bibliographic analysis using DL for solar forecasting.

Ref.	Year	Method	Data Used	Performance Metrics
[19]	2021	SCNN–LSTM	NREL's Solar Radiation Research Laboratory (SRRL)	*NRMSE* = 23.47% nMAE = 13.75%
[21]	2019	LSTM–RNN	Aswan (Dataset1) and Cairo (Dataset2) cities, Egypt.	82.15 (*RMSE*)
[22]	2019	DRNN–LSTM	Sails in the Desert, Yulara, Australia.	DRNN–LSTM: 7.53 (*RMSE*), 4.369 (*MAE*), 15.87% (*MAPE*)
[23]	2018	VMD–CNN	An electric power company in Jiangsu Province, China.	1.5418 (*MAPE*), 2.0533 (*RMSE*), 0.1752 (*MAE*)
[24]	2020	CNN LSTM	Data is taken from 500 kWp PV plant in Taiwan [25]	CNN: 29.72% (*MAPE*), 2.94% (MRE) and for LSTM: 35.85% (*MAPE*), 5.99% (MRE).
[26]	2020	LSTM	Datset1: Brazilian data Datset2: Spanish data	*MAPE*: 7.19% (LSTM)
[27]	2021	Hybrid CSO (Chicken Swarm Optimization)-GWO (Grey Wolf Optimization)	The Photo-Voltaic Graphical Information System—Surface Solar Radiation Dataset Heliosat (PVGIS-SARAH)	R^2 = 0.9731
[28]	2021	Hybrid LSTMconv	www.soda-pro.com (accessed on 21 May 2021)	*MAE* = 66.75%(ULM) *MAE* = 62.87%(Hull)

The following are the few major contributions of the work:

i. This article provides a brief literature study on state-of-the-art solar power prediction methods, their advantage/disadvantages, and the research gap available.
ii. This article presents a novel hybrid multistep CNN stacked LSTM with a drop-out model for the prediction of solar irradiance. Moreover, the POA irradiance is also forecasted as a novel application. The proposed stacked architecture and the incorporation of drop-out layers are helpful for accuracy improvement in the PV prediction model.
iii. Multi-step CNN layers helped to extract features from the data and to produce sequenced data. The stacked LSTM effectively collects this data, forecasts it to improve prediction accuracy.
iv. At last, the performance of the proposed solar prediction model has been validated through a detailed comparative analysis with several other contemporary ML and DL approaches such as artificial neural network and traditional LSTM model for *RMSE*, *MAE*, *MAPE*, R^2, *MSE*, and NMSE. Moreover, the output of several other works that published recently are also compared with the outcome of the proposed approach.

The subsequent sections of this article are presented as: Data Description is given in Section 2; Proposed methodology is presented in Section 3, result and analysis with comparative discussion is presented in Section 4 and lastly, Section 5 concludes the manuscript.

2. Data Description and Data Preprocessing

From the literature, it can be analyzed that most of the past studies (related to solar PV projects) have used irradiance as a key variable for solar forecasting. However, effective measurement of the irradiance requires expensive sensors and other equipment [4,5]. In contrast, POA irradiance can be considered as an alternative measure for solar prediction since it is inexpensive, does not necessitate any additional machinery, and is easier than beam or diffuse irradiance. In this regard, two different sets of solar time-series data (irradiance and POA) are used for the testing and validation of the proposed approach. These data are collected from the Sweihan Photovoltaic Independent Power Project in Abu Dhabi during July 2019. Here, the solar irradiance dataset is formulated using the pyranometer and the sensor output voltage (refer to Equation (1)).

$$E_{solar} = \frac{U_{emf}}{S} \tag{1}$$

where U_{emf} denotes the sensor output voltage (unit: μV), S means for sensitivity (unit: μV/W/m^2), and E_{solar} means for solar irradiance (unit: W/m^2). Figure 2a,b show the distribution of real-time solar irradiance and POA irradiance data, respectively, from Sweihan Photovoltaic Independent Power Project in Abu Dhabi.

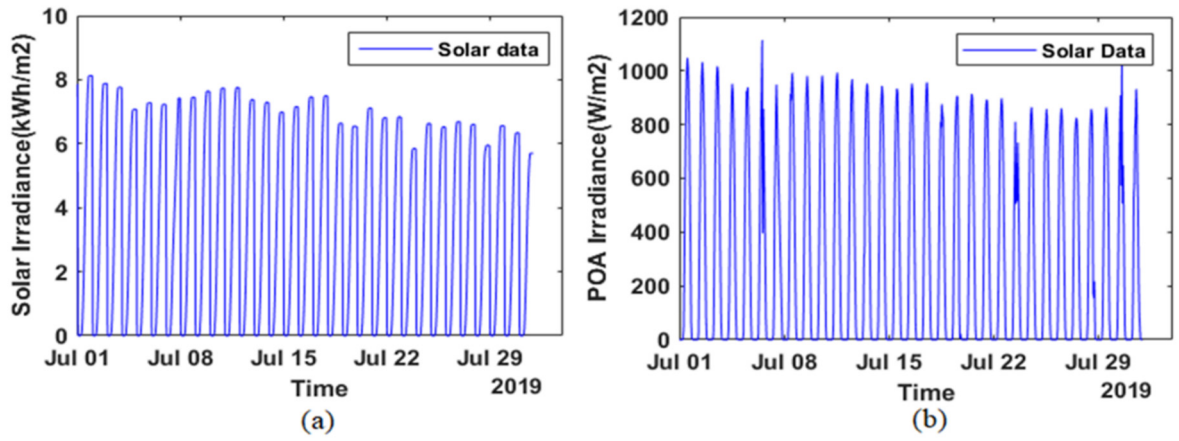

Figure 2. Distribution of solar irradiance: (**a**) Solar Irradiance; (**b**) POA Sweihan Photovoltaic Independent Power Project.

It is seen that irradiance varied from 0 to 8.12 (kWh/m^2) and POA varied from 0 to 1114 (W/m^2). In this work, the total collected data is divided into a 7:3 ratio for the training and testing of the proposed model. The observed data were partitioned into training and testing data to use the deep learning technology for solar forecasting, and the data division evaluated in this research work covers 70–30%. Deep learning algorithms also respond differently depending on the size of the data set used in the training and testing phases. The incident solar irradiance data has a lot of variables, and because it has so many dimensions, it needs to be scaled before it can be fed into a deep learning network. This section elaborates on the data standardization procedure that was utilized to prepare the data. Rescaling the data set so that the mean of the observed values is 0 and the standard deviation is 1 is called data standardization. It is calculated in the following manner.

$$x_{std} = \frac{x - mean(x)}{std_{dev}} \tag{2}$$

where, x is the sample, $mean(x)$ represents the mean of the sample, and std_{dev} represents the corresponding standard deviation.

3. Methodology

In this work, two different kinds of DL techniques (such as CNN and LSTM) and a proposed hybrid multi-step CNN-LSTM are utilized for short-term solar energy prediction. Afterward, these models are evaluated and compared through training and validation performance. Brief literature of these methods is presented below.

3.1. CNN

CNN is a widely used kind of deep learning technology for picture, text, and signal inputs. The design of a CNN is determined by the types and number of layers it comprises, such as convolutional layers, pooling layers, and fully connected layers, and is inspired by the genetic structure of a visual cortex, which has configurations of simple and complicated cells [29]. Initially, the input data is fed to the input layer to process it for feature transformation. Then, feature extraction is carried out in the convolution and pooling layers. Afterward, these extracted information yields from convolution and pooling layers are assimilated by the fully-connected layers. Finally, the output result is communicated through the output layer. A pictorial basic architecture is portrayed in Figure 3 [30].

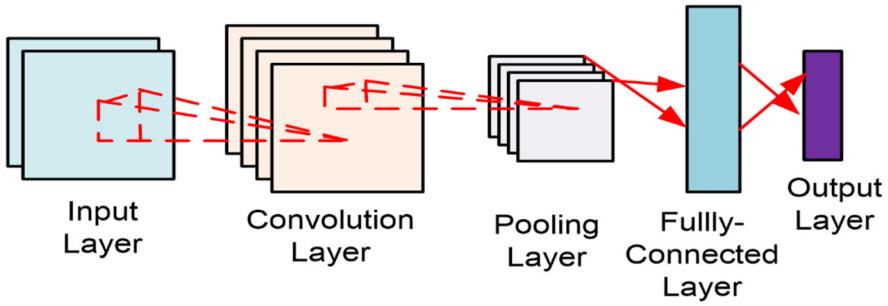

Figure 3. Architecture of CNN.

The convolution layer plays a very vital role in the CNN architecture as it is used to extract the features/information from input data through convolution kernels. The usual size of the input matrix is generally larger than the convolution kernels. A convolution layer uses a convolution operation rather than a universal matrix operation for the feature mapping task. Each element in the feature map is given by,

$$S_{i,j}^{out} = f_{con}\left(\sum_{x=0}^{p}\sum_{y=0}^{p} w_{x,y} s_{i+x,j+y}^{in} + b\right) \tag{3}$$

where $S_{i,j}^{out}$ stands for an output value of the feature map. $s_{i+x,j+y}^{in}$ signifies the input matrix. f_{con} is carefully chosen activation function. $w_{x,y}$, b denotes the weight and bias of the convolution kernel. The pooling layer decreases the dimensions of the prior feature map and enhances the efficacy of the computation process through down-sampling. Finally, the fully-connected layer is used to flatten the features, which are generated by the convolution and pooling layer and unites them to acquire the final output result.

3.2. LSTM

To compensate for the vanishing gradient problem of RNN, LSTM models were developed [31]. LSTM model is suitable to classify the process and forecast the time-series data. The architecture of the LSTM unit is displayed in Figure 4 [32]. A memory cell is a central segment of the memory unit (denoted by the green circle in Figure 4), which is utilized to store past information. The input stands for the known time-series data and the output signifies the prediction output (denoted as 'O_t'). Fundamentally, the memory unit is comprised of a cell state and three gates such as an input gate, an output gate, and a forget gate. The gates are indicated by blue circles in Figure 4. The cell state is the channel to transmit the information in sequential order. The function of the gates is to update or reject past information. The cell state is specified by S_t. X_t is the pre-processed data, which is fed as input data. The previous state of the memory cell is designated by S_{t-1}. The red circles in Figure 4 refer to union points/confluences, basically multiplication. The dashed lines are meant for the functions of the previous state. Considering the type of flow of information in the memory unit, the state of the cell gets updated. Equation (4) shows the derivation of LSTM [32].

$$\left.\begin{array}{c} i_t = \sigma\left(W^{(i)}X_t + Z^{(i)}S_{t-1}\right) \\ f_t = \sigma\left(W^{(f)}X_t + Z^{(f)}S_{t-1}\right) \\ O_t = \sigma\left(W^{(o)}X_t + Z^{(o)}S_{t-1}\right) \\ S^{\sim}{}_t = \tanh\left(W^{(c)}X_t + Z^{(c)}S_{t-1}\right) \\ S_t = f_t{}^o S_{t-1} + i_t{}^o S_t \\ O_t = O_t{}^o \tanh(S_t) \end{array}\right\} \quad (4)$$

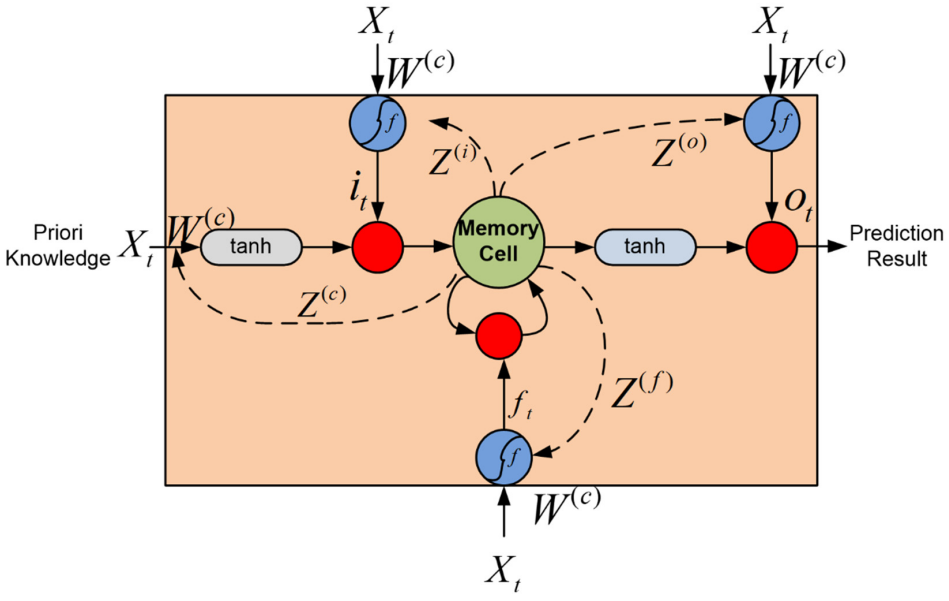

Figure 4. Architecture of LSTM.

Here, in (4), the following few lines describe the abbreviation and symbol for a better understanding of the reader. The symbol "o" stands for the Hadamard product. i_t, f_t, and O_t are the output of input, forget and output gates, respectively. $S^{\sim}{}_t$ and S_t are updated

and final state of the memory cell. O_t is the final output of the memory unit. $W^{(i)}$, $W^{(f)}$, $W^{(o)}$, $W^{(c)}$, $Z^{(i)}$, $Z^{(f)}$, $Z^{(o)}$, $Z^{(c)}$ are the coefficient matrixes (as labeled in Figure 4 through functions of the different gates). In contrast to RNN, the LSTM can capture the complex correlation features within the time-series data in both the short and long term.

3.3. Proposed Multistep CNN-Stacked LSTM Model

Since traditional CNN approaches have a lengthy prediction time and reduced accuracy, hybrid models for forecasting problems had been developed. Hybridization of CNN with LSTM might be considered as one of the solutions to these issues. The hybrid CNN-LSTM architecture was used to predict time-series in a variety of applications in diverse domains, for example, environmental quality prediction [30,33], solar energy prediction [34], wind speed prediction [35], domestic loads forecasting [36,37], etc. As a hybrid model, various researchers have suggested numerous combinations of modes of the CNN-LSTM. The proposed multistep CNN-stacked LSTM in this work has the advantage of detecting features from the input time series data before passing them on to the stacked LSTM. In our suggested multistep CNN-stacked LSTM with drop-out layer, the CNN and stacked LSTM is integrated so that the input data features are processed using CNN and are fed into stacked LSTM layers. Table 2 shows the different layers considered for multi-step CNN stacked architecture and its functions. Figure 5 shows the detailed architecture.

Table 2. Multi step-CNN stacked layers and their functions.

No.	Layer	Function
1	Sequence Input Layer	Inputs sequence data to a network.
2	Sequence Folding Layer	The batch of data sequences is transformed into a batch of data
3	Convolution2dLayer	Sliding filters are applied to the input.
4	Relu Layer	Every element of the input is subjected to a threshold operation.
5	averagePooling2dLayer	Down samples the input by splitting it into rectangular pooling zones and calculating the average values of each.
6	Sequence Unfolding Layer	Re-establish the input data's sequence architecture after the sequence folding layer.
7	Flatten layer	A flatten layer reduces the input's spatial size to the channel size.
8	LSTM layer	In time-series data, the LSTM layer acquires long-term dependencies between time steps.
9	Drop out layer	With a certain probability, the dropout layer transforms input elements to zero randomly.
10	Fully Connected Layer	A fully connected layer outputs the prediction
11	Regression Layer	Evaluate the half-mean-squared-error loss.

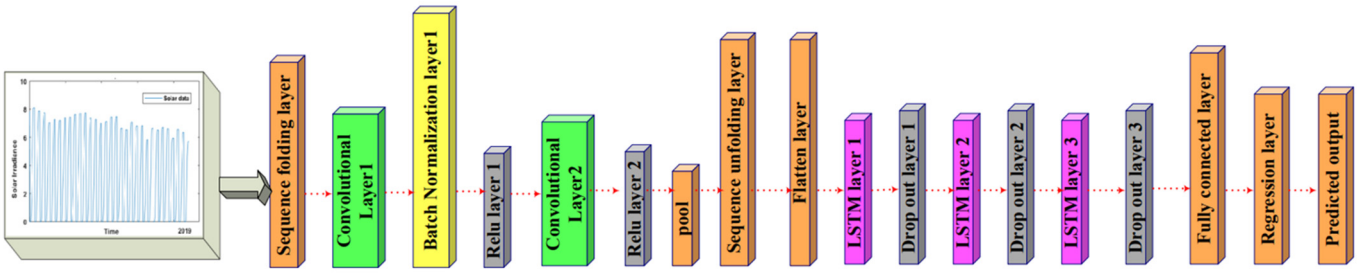

Figure 5. Multistep CNN stacked LSTM.

The architecture employed in this study contains two phases of convolution, i.e., two layers of convolution with relu layers. To combine CNN and LSTM, a folding layer was added after the sequence input layer. A batch of data sequences was transformed into a

batch of data via the sequence folding layer. The CNN comes into action after this layer. A sequence unfolding layer was employed after the CNN to turn the batch of data into a batch of sequenced data. The sequence data is the stacked LSTM's input. The stacking of various LSTM layers for a deep LSTM based neural network is significant in neural network model learning since higher LSTM layers can record theoretical concepts in series, improving forecasting results. "Each hidden unit in a neural network trained with dropout must learn to work with a randomly chosen sample of other units", according to Srivastava et al. [38]. There is a flatten layer before the stacked LSTM layer that reshapes the input data to the LSTM layer's input. Here, we used three stages of LSTM layers with the drop-out layer having the value 0.1006 to avoid overfitting. Finally, the output with the regression layer is shown in Figure 5. Table 3 details the architecture of the proposed network with the number of filters, filter sizes, and layers used in the proposed model.

Table 3. The architecture of the proposed multi step-CNN stacked LSTM network.

Group	Parameter	Value	Description
Sequence folding layer			
Conv2DLayer 1	filters	256	Filter size = 5 × 5
Batch normalization layer			
Relu layer			
Conv2DLayer 2	filters	256	Filter size = 5 × 5
Averagepoolng2D layer			Filter size = 5 × 5
Sequence unfolding layer			
Flatten layer			
LSTM layer1	No: of hidden units = 100	Drop out = 0.1	
LSTM layer2	No: of hidden units = 100	Drop out = 0.1	
LSTM layer3	No: of hidden units = 300	Drop out = 0.1	
Fully connected layer			
Regression layer			
Training	Optimizer	ADAM optimizer	
Training	Mini batch size	64	
Training	Learning rate	0.00501	Learning rate of optimizer

4. Result and Analysis

The major objective of this work is to study the performance of the three DL-based prediction techniques for instance LSTM, CNN, and the proposed hybrid multistep CNN-stacked LSTM models, to forecast the solar energy variables (Irradiance and POA). Moreover, few traditional machine learning models are also tested and compared with the proposed approach. To check the feasibility, the case studies included two models of data, which are solar irradiance data from Sweihan PV Independent Power Project and POA data from Sweihan PV Independent Power Project, UAE. Forecasting performances are evaluated by considering various performance metrics (visit Section 4.1 for details), and their values are given under each case study, respectively. For each case study, the data was divided into 70–30% proportions. Simulations and programming have been conducted in a MATLAB environment.

4.1. Model Performance Measure

As mentioned above, the following measuring indices are used in this work to validate the performance of the prediction model such as Mean Absolute Error (*MAE*), Coefficient of Determination (R^2), Mean Squared Error (*MSE*), Root Mean Square Error (*RMSE*), Mean Absolute Percentage Error (*MAPE*), and Normalized Root Mean Squared Error (*NRMSE*) are considered for evaluating the performance. The relatively lower values of these measures suggest better prediction. In the below-detailed metrics, n is the number of samples, F is the forecasted value, and O_b is the observed value.

(a) Mean Absolute Error (*MAE*): The *MAE* has been frequently utilized to solve regression problems and to examine forecast performance in the renewable energy industry. It is the absolute value of the difference between the forecast value and the observed value.

$$MAE = \frac{1}{n}\sum_{i=1}^{n}|F_i - O_{bi}| \tag{5}$$

(b) Root Mean Square Error (*RMSE*): The *RMSE* is the square root of the average of squared differences between forecast and observed values. *RMSE* is given by:

$$RMSE = \sqrt{\left(\frac{1}{n}\sum_{i=1}^{n}(F_{i-}O_{bi})^{2}\right)} \tag{6}$$

RMSE is a commonly used metric for evaluating solar forecasting accuracy. The errors are squared before they are averaged and hence it gives higher weight to large errors. When analyzing forecasts in circumstances where significant mistakes are undesired, the *RMSE* is used.

(c) Mean Absolute Percentage Error (*MAPE*): It is the mean or average of the absolute percentage errors of forecasts.

$$MAPE = \frac{1}{n}\sum_{i=1}^{n}\left|\frac{F_{i-}O_{bi}}{O_{bi}}\right| * 100 \tag{7}$$

(d) Coefficient of Determination (R^2)*:* The Coefficient of Determination measures the extent that variability in the forecast errors is explained by variability in the observed values. The formula R^2 is as follows.

$$R^2 = 1 - \frac{\sum_{i=1}^{n}(F_i - O_{bi})^2}{\sum_{i=1}^{n}(F_i - \overline{O_{bi}})^2} \tag{8}$$

where $\overline{O_{bi}}$ is the mean value of observations. When the value R^2 is close to one, the predicting accuracy improves.

(e) Mean Squared Error (*MSE*): It measures the average of the squares of the errors and is given by,

$$MSE = \frac{1}{n}\sum_{i=1}^{n}(F_i - O_{bi})^2 \tag{9}$$

(f) Normalized Root Mean Squared Error (*NRMSE*): The *NRMSE* is the normalized form of the *RMSE*.

$$NRMSE = \frac{RMSE}{mean(Observedvalues)} = \sqrt{\sum_{i=11}^{n}\frac{(F_{i-}O_{bi})^{2}}{O_{bi}}} * 100\ \text{kWh/m}^2 \tag{10}$$

4.2. Case Study-I: Solar Irradiance-Sweihan Photovoltaic Independent Power Project, Abu Dhabi

In this section, the collected solar irradiance GHI irradiance GHI kWh/m^2 from from Sweihan Photovoltaic Independent Power Project was used to evaluate the performance of the proposed architecture. As this is a univariate analysis, we considered a single column of solar irradiance GHI for July 2019. The observed values of solar irradiance were compared with predicted values, as shown in Figures 6–8 with error values for CNN, LSTM, and multistep CNN stacked LSTM. It gives an insight into the performances of all different architectures discussed so far. The performance accuracy and flexibility in selecting the input variables are examined in Table 4 using the six-error metrics as detailed previously.

The closer the value R^2 to 1, the more accurate the model is. From Table 4, it can be easily analyzed that the CNN architecture performed the prediction task with the error matrices such as RSME: 0.98, *MSE*: 0.78, *MAPE*: 14.48, R^2 = 0.87, *MSE* = 0.99, and *NRMSE* = 0.31. However, the LSTM model performs better compared with CNN with error matrices such as RSME: 0.90, *MSE*: 0.40, *MAPE*: 9.20, R^2 = 0.90, *MSE* = 0.82, and *NRMSE* = 0.29. Lastly, it can be analyzed that the proposed multistep CNN stacked LSTM model outperforms other previously stated DL model for all performance matrices. The performance results are noted as RSME: 0.36, *MSE*: 0.18, *MAPE*: 3.11, R^2 = 0.98, *MSE* = 0.13, and *NRMSE* = 0.11.

Table 4. Comparison of different DL architectures utilizing solar irradiance data.

Architecture	*RMSE*	*MAE*	*MAPE*	R^2	*MSE*	*NRMSE*
CNN	0.98	0.78	14.48	0.87	0.99	0.31
LSTM	0.90	0.40	9.20	0.90	0.82	0.29
Multi step CNN Stacked LSTM	0.36	0.18	3.11	0.98	0.13	0.11

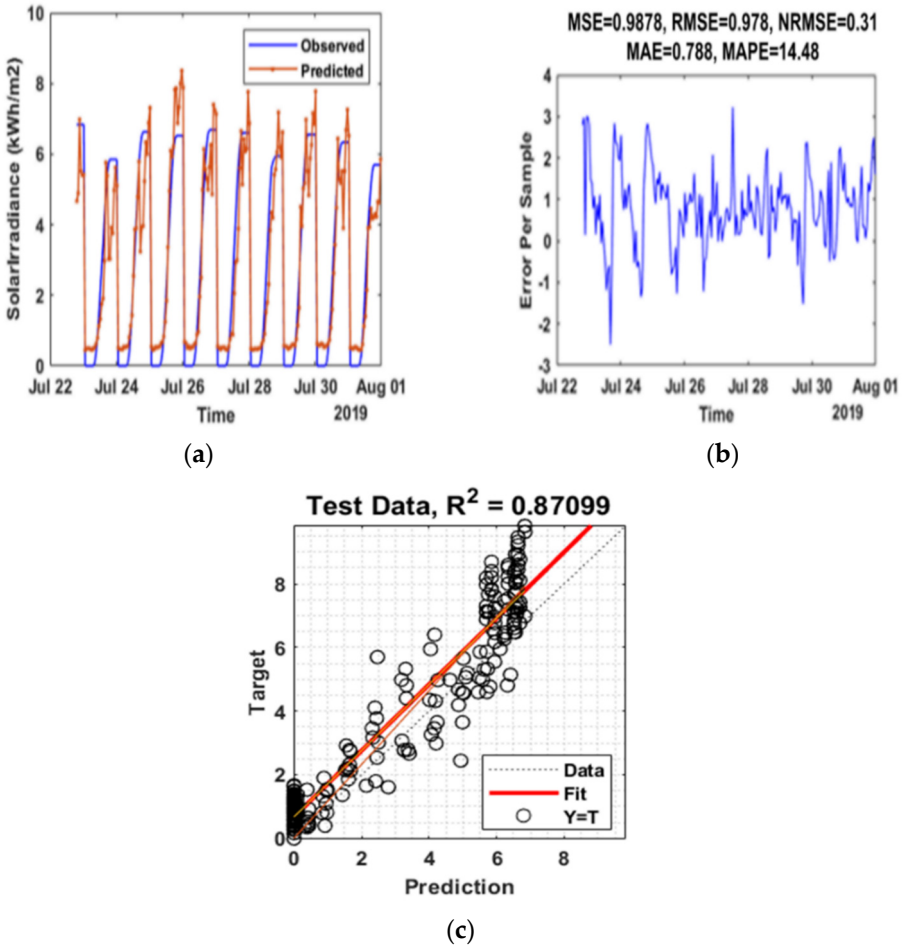

Figure 6. (**a**) The observed and predicted results, (**b**) error metrics and (**c**) regression plot considering solar irradiance-Sweihan photovoltaic independent power project, Abu Dhabi-for CNN.

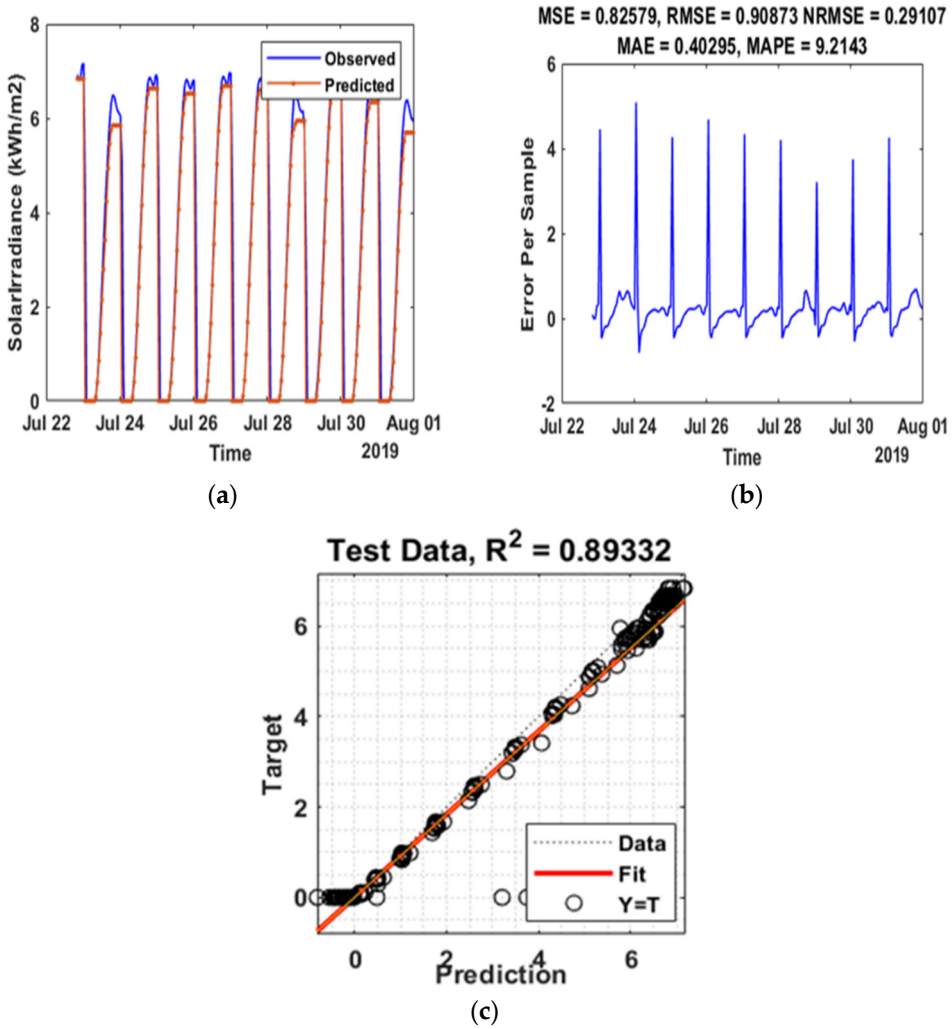

Figure 7. (**a**) The observed and predicted results, (**b**) error metrics and (**c**) regression plot considering solar irradiance-Sweihan photovoltaic independent power project, Abu Dhabi-for LSTM.

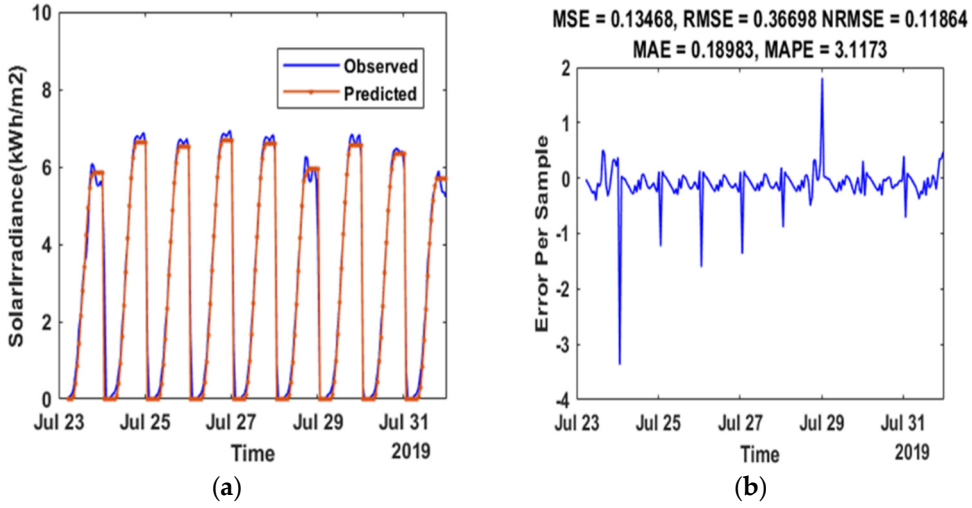

Figure 8. *Cont*.

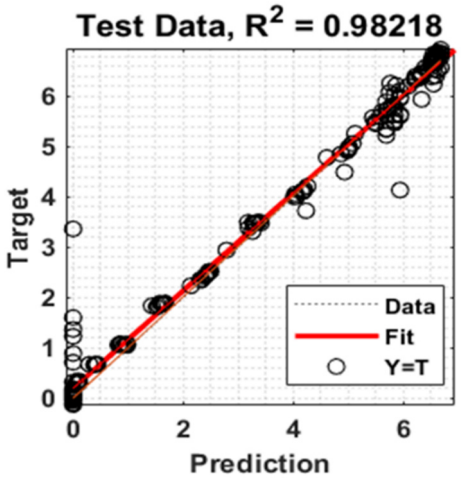

(**c**)

Figure 8. (**a**) The observed and predicted results, (**b**) error metrics and (**c**) regression plot considering solar irradiance-Sweihan photovoltaic independent power project, Abu Dhabi-for Multistep CNN-stacked LSTM.

4.3. Case Study-II: POA_Sweihan Photovoltaic Independent Power Project, Abu Dhabi

In this subsection, the forecasting performance of the proposed model is evaluated using POA irradiance. Prediction accuracy depends on the accuracy of all-weather forecasting variables. Even after incorporating POA data, it was seen that the error metrics are comparable with the results obtained by using solar irradiance GHI data. The observed values of POA irradiance are compared with predicted values, as shown in Figures 9–11 with error values for CNN, LSTM, and multistep CNN stacked LSTM, respectively. The performance accuracy and flexibility in selecting the input variables are examined in Table 5 using the six-error metrics as detailed previously. From Table 5, it can be easily analyzed that the CNN architecture performed the prediction task with the error matrices such as RSME: 78.50, *MSE*: 58.90, *MAPE*: 14.70, R^2 = 0.94, *MSE* = 6173, and *NRMSE* = 0.30. However, the LSTM model performs better compared with CNN with error matrices such as RSME: 72.40, *MSE*: 38.00, *MAPE*: 9.00, R^2 = 0.95, *MSE* = 5254, and *NRMSE* = 0.27. Lastly, it can be analyzed that the proposed multistep CNN stacked LSTM model outperform other previously stated DL model concerning all performance matrices. The performance results are noted as RSME: 61.24, *MSE*: 29.00, *MAPE*: 6.70, R^2 = 0.96, *MSE* = 3750, and *NRMSE* = 0.22.

Table 5. Comparison of different DL architectures utilizing POA irradiance data.

Architecture	*RMSE*	*MAE*	*MAPE*	R^2	*MSE*	*NRMSE*
CNN	78.50	58.90	14.70	0.94	6173	0.30
LSTM	72.40	38.00	9.00	0.95	5254	0.27
Multi step CNN Stacked LSTM	61.24	29.00	6.70	0.96	3750	0.22

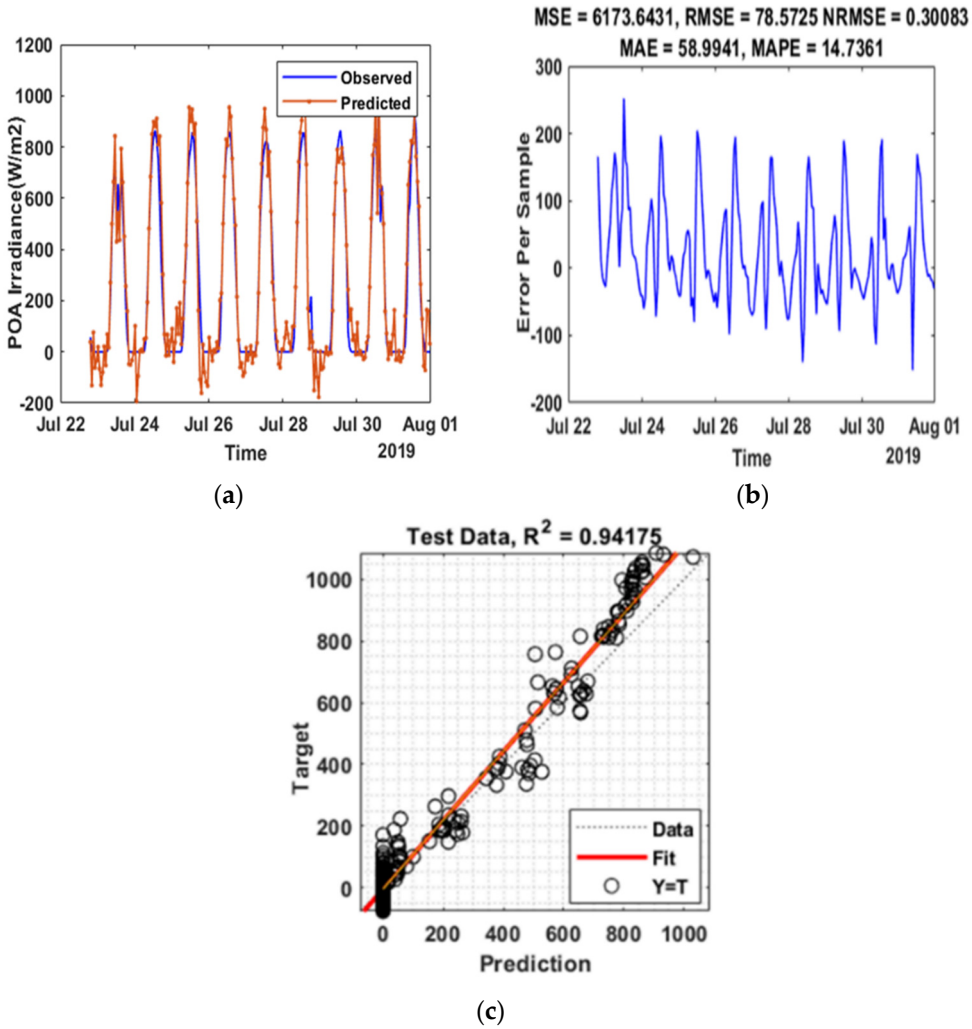

Figure 9. (**a**) The observed and predicted results, (**b**) error metrics and (**c**) regression plot considering POA-Sweihan photovoltaic independent power project, Abu Dhabi, for CNN.

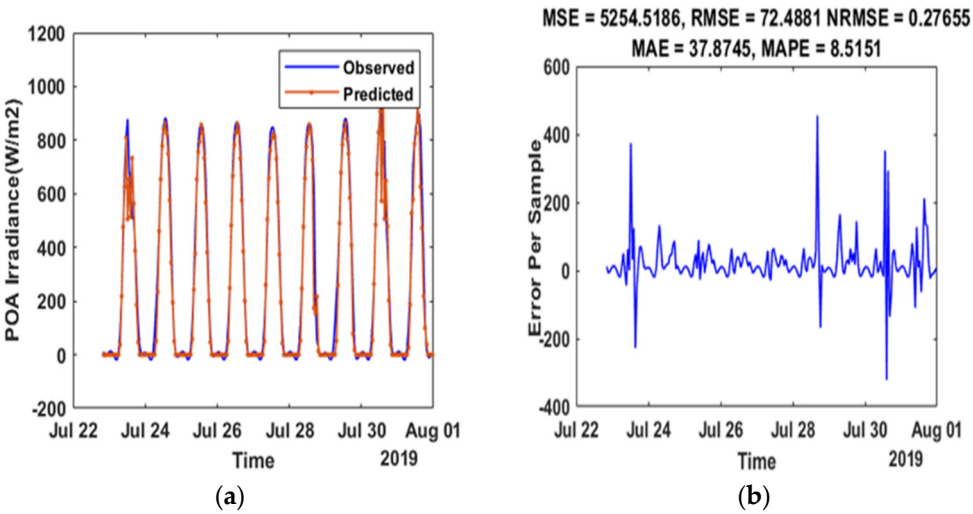

Figure 10. *Cont*.

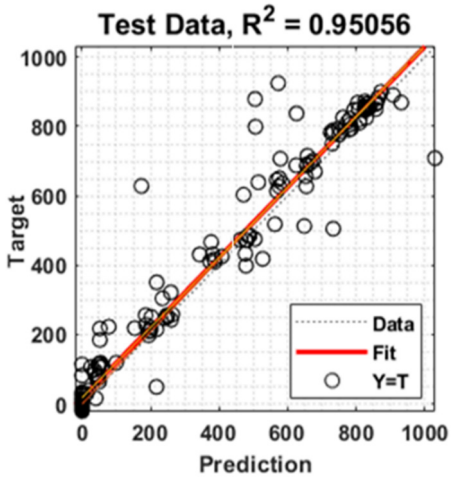

(**c**)

Figure 10. (**a**) The observed and predicted results, (**b**) error metrics and (**c**) regression plot considering POA—Sweihan photovoltaic independent power project, Abu Dhabi, for LSTM.

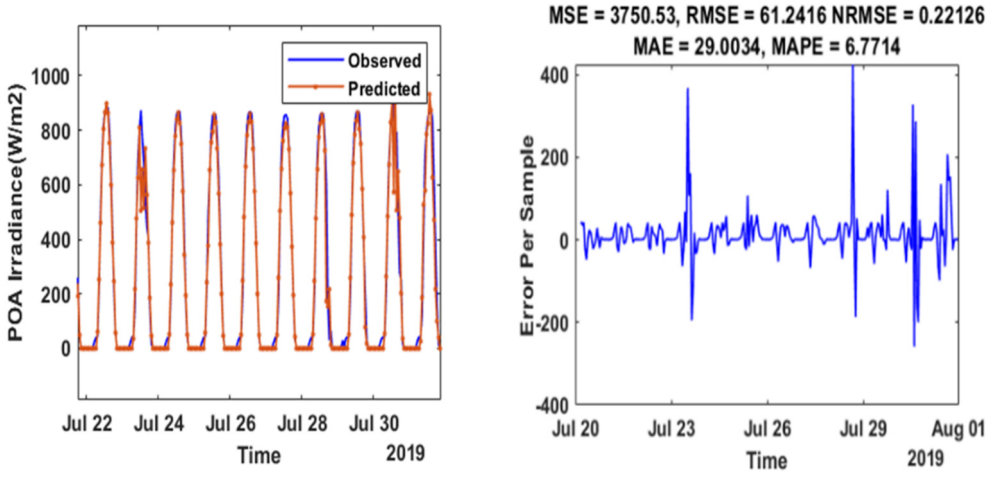

(**a**) (**b**)

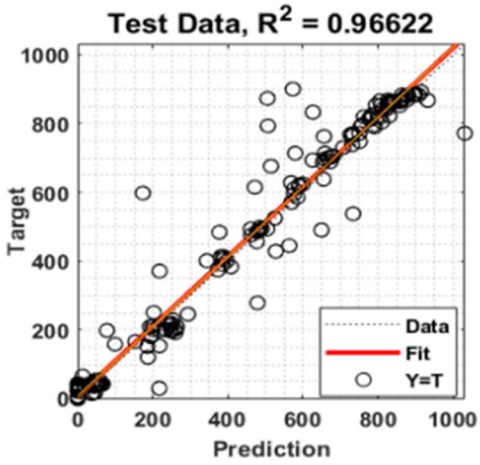

(**c**)

Figure 11. (**a**) The observed and predicted results, (**b**) error metrics and (**c**) regression plot considering POA—Sweihan photovoltaic independent power project, Abu Dhabi, for Multistep CNN-stacked LSTM.

4.4. Critical Analysis

In this work, the authors proposed a novel Multi-step CNN-stacked LSTM model with a drop-out layer for short-term solar irradiance and POA irradiance prediction. The result as presented in the previous subsection indicates the efficacy of the proposed approach in terms of all performance measures. To justify the result accuracy, the output result of the proposed approach is compared with CNN and LSTM model individually considering both the data, where it is seen that the proposed approach outperforms the contemporary DL models. Again, to show a clear picture of the performance of the proposed approach, an extended analysis is carried out in this section including a comparative study with state-of-the-art ML techniques and recently published DL techniques. Furthermore, the robustness of the proposed architecture with noise-injected data is presented below in the subsequent section.

4.4.1. Comparative Analysis with the State-of-the-Art Techniques

In this subsection, the performance of the proposed method is compared with the state-of-the-art ML techniques such as Linear Regression (LR), Support Vector Regression (SVR), and (ANN) with the same data set. LR is a Supervised Learning Algorithm (SLA) used to predict the continuous values based on an input data vector (x). From a geometrical viewpoint, each data sample is considered as a point. LR aims to determine the parameters (β_0 and β) of the linear function ($y = \beta_0 + x^T\beta$), so the distance amongst all the points and the line is as lesser as possible [39]. Here, y is the prediction value. A gradient descent search algorithm is used to update the parameters. Similar to LR, SVR is also a supervised-ML model used to learn the underlying patterns [40]. In the last few decades, the SVR model is popularly used in developing prediction algorithms [41,42]. SVR executes the structural risk minimization inductive principle to achieve fair generalization on a restricted number of learning points, i.e., reducing the global error bound rather than minimizing perceived training error. The support vector regressor is based on the computation of an LR function in a large dimensional feature space. The detailed description of SVR can be followed from [42]. Here, the required parameters used for initializing the model are as follows: Kernal: RBF, Gamma: 0.000007, and trade-off parameter (C): 620. Similar to LR and SVR, the ANN is also a supervised-ML model used for classification and regression. The ANNs are tuned to fulfil a necessary mapping of input data to the outputs using training algorithms. The most common training algorithm used for the feed-forward neural network is the error back-propagation. It is a supervised training method, as the target outputs are also fed to NN during training together with the input data. In this work, the required parameters used to initialize the ANN model are as follows: Hidden layer neurons: six, activation functions: 'tansig', and the maximum number of epochs: 100. The whole comparative result is presented in Figure 12. The bar graph shows the value of *NRMSE* as obtained from the comparative methods. Here, the superiority of the proposed multistep CNN-Stacked LSTM model can be analyzed. It is observed that the proposed method achieved better solar irradiance forecasting accuracy. The comparative study in the literature is given in Table 6. It summarizes the forecasting performance of several hybrid networks with their performance metrics, whereby the accuracy of the proposed method is highlighted in bold letters. Furthermore, the literature results given in Table 6 shows that the errors are not significantly smaller.

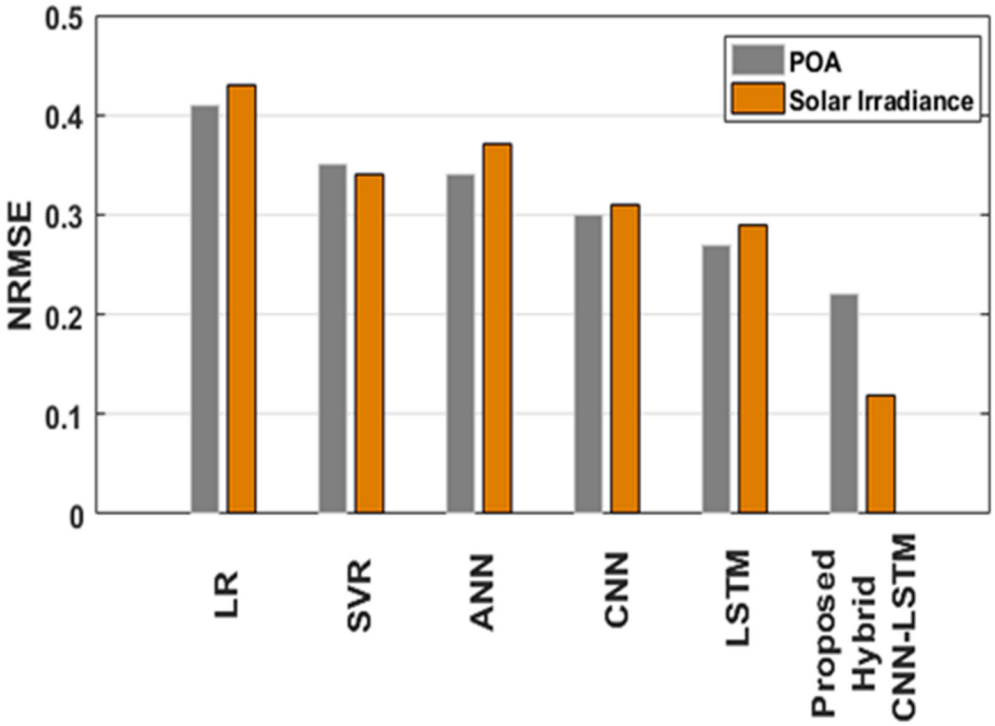

Figure 12. Comparative result.

Table 6. Comparison of the results of the study method with the state of the art.

Ref.	Year	Method	Country	Lowest Error
[16]	2019	DNN models (LSTM, CNN)	Taiwan	*RMSE* = 126.91–140.9
[21]	2017	5 different LSTM architectures	Egypt	*RMSE*: 82.15–136.87
[34]	2020	CEEMDAN-CNN-LSTM	Los Anegles	*RMSE* = 34.72 *NRMSE* = 12.19
[43]	2020	DNN models (LSTM, CNN LSTM, Conv LSTM)	Fuhai, Taiwan	R^2 = 0.54–0.7 *RMSE* = 0.18–0.2
[44]	2020	Hybrid LSTM	Limberg, Belgium	*RMSE* = 6.4 R^2 = 0.95–0.98
[45]	2020	LSTM	Gujarat, India	*RMSE* = 11.6
[46]	2020	Solar Net model (Deep CNN)	Golden Colerado	*RMSE* = 116.82 *NRMSE* = 8.85%
[47]	2020	CNN-LSTM	Dallas	*RMSE* = 97.10 *NRMSE* = 24.53
[48]	2021	CNN-LSTM	Morocco	*RMSE* = 8.6
[49]	2021	LSTM-CNN	San Diego	*RMSE* = 42.89
Proposed work: Multistep CNN Stacked LSTM			Abu Dhabi	*NRMSE* = 0.11 *RMSE* = 0.36

4.4.2. Robustness of the Proposed Architecture under Noise-Injected Data

To verify the robustness of the proposed architecture, with noise-injected data, this study used the Gaussian noise produced in MATLAB. Gaussian noise with standard deviation equal to one and mean equal to zero is injected. Finally, the results are evaluated with performance metrics, thereby analyzing the noise impact to validate the functionality and efficiency of the proposed method. In this study, the impact of noise injection on the model performance is presented. The noise is injected into the testing data subset with different percentages, i.e., 0, 50, and 100%, and the performance differences of the proposed method for 50SNR (Signal to Noise Ratio) and 32 SNR are examined in detail [50,51]. From

Tables 7 and 8, it is observed that the proposed Multi-Step CNN Stacked LSTM Technique achieved comparable performance even with noise-injected data sets.

Table 7. Robustness Analysis of the proposed Multi-Step CNN Stacked LSTM Technique with 50 dB SNR.

Error Metrics	0% (No Noise Is Injected)	50% (Noise Injected to 50% of Data)	100% (Noise Injected to 100% of Data)
RMSE	0.36	0.3670	0.3930
MAE	0.18	0.1898	0.1922
MAPE	3.11	3.1173	2.8315
R^2	0.98	0.9822	0.9795
MSE	0.13	0.1347	0.1545
NRMSE	0.11	0.1186	0.1260

Table 8. Robustness Analysis of the proposed Multi-Step CNN Stacked LSTM Technique with 32 dB SNR.

Error Metrics	0% (No Noise Is Injected)	50% (Noise Injected to 50% of Data)	100% (Noise Injected to 100% of Data)
RMSE	0.36	0.367	0.75
MAE	0.18	0.189	0.41
MAPE	3.11	3.11	6.19
R^2	0.98	0.98	0.93
MSE	0.13	0.1347	0.57
NRMSE	0.11	0.1186	0.23

5. Conclusions

In this study, a Multi-step CNN Stacked LSTM technique is proposed to predict two easily measured solar energy variables, i.e., solar irradiance and POA irradiance. First, a multi-step CNN was built with multiple layers by improving traditional CNN, which independently extracts features from the observed data. The sequenced output data was fed to stacked LSTM with drop-out architecture to output the target variable without overfitting. Solar data were collected at one-hour intervals for July 2019 from the Sweihan photovoltaic independent power project, Abu Dhabi. The input dataset was transformed into a supervised frame and then split into training (70%) and testing (30%) datasets. In the testing period, the data were fed as input to evaluate the performance of the models utilizing statistical measures: *RMSE*, *MAE*, *MAPE*, R^2, *MSE*, and *NRMSE*. Here, the LSTM outperformed the CNN in predicting solar irradiance and POA. However, the hybrid multistep CNN-stacked LSTM model proved to be stronger compared to both standalone DL models, confirmed that it reduced the *RMSE* for solar irradiance prediction was 0.36 with R^2 0.98, and for POA prediction was 61.24 with R^2 0.96. Lastly, the results are also compared with the state-of-the-art ML model, where the superiority of the DL model over the ML model in terms of prediction accuracy is justified. Future work will focus on the further improvement in the performance of the proposed model; moreover, fine-tuning of other significant parameters also can be considered. As a result, additional datasets will be used to investigate the model in more depth, and it will be tested independently in as many locations as possible.

Author Contributions: N.E.M.: methodology, software, validation, data curation, investigation, and formal analysis; M.M.: writing—original draft preparation, validation, and formal analysis; S.H.: conceptualization, methodology, writing review, editing, and supervision; A.A.-D.: writing—review and editing, validation, formal analysis, and resources. All authors have read and agreed to the published version of the manuscript.

Funding: This research/publication is based upon work supported by the Birla Institute of Technology and Science Pilani, Dubai Campus.

Institutional Review Board Statement: Not applicable.

Informed Consent Statement: Not applicable.

Acknowledgments: We acknowledge the data received from the Sweihan Photovoltaic Independent Power Project in Abu Dhabi. The validation of the proposed model was made possible using real-time data from the Sweihan Photovoltaic Independent Power Project.

Conflicts of Interest: The authors declare that they have no known competing financial interests or personal relationships that could have appeared to influence the work reported in this paper.

Abbreviations

The following abbreviations are used in this manuscript:

ANN	Artificial Neural Network
CNN	Convolutional Neural Network
CSO	Chicken Swarm Optimization
DBN	Deep Belief Network
DCNN	Deep Convolutional Neural Network
DL	Deep Learning
ELM	Extreme Learning Machine
GHI	Global Horizontal Irradiance
GWO	Grey Wolf Optimization
LR	Linear Regression
LSTM	Long-Short-Term-Memory Network
MAE	Mean Absolute Error
MAPE	Mean Absolute Percentage Error
ML	Machine Learning
MLP	Multi-Layer Perceptron
MSE	Mean Squared Error
NRME	Normalized Root Mean Squared Error
POA	Plane of Array
RES	Renewable Energy Sources
RMSE	Root Mean Square Error
RNN	Recurrent Neural Network
SLR	Supervised Learning Algorithm
SNR	Signal to Noise Ratio
SRRL	Solar Radiation Research Laboratory
SPR	Support Vector Regression
SPV	Solar Photo Voltaic
SVM	Support Vector Machine
SVR	Support Vector Regression

References

1. Swain, M.K.; Mishra, M.; Bansal, R.C.; Hasan, S. A Self-Powered Solar Panel Automated Cleaning System: Design and Testing Analysis. *Electr. Power Compon. Syst.* **2021**, *49*, 308–320. [CrossRef]
2. Murdock, H.E.; Gibb, D.; Andre, T.; Sawin, J.L.; Brown, A.; Ranalder, L.; Collier, U.; Dent, C.; Epp, B.; Hareesh Kumar, C.; et al. Renewables 2021-Global Status Report. Available online: https://www.ren21.net/wp-content/uploads/2019/05/GSR2021_Full_Report.pdf (accessed on 8 February 2022).
3. Carrière, T.; Amaro e Silva, R.; Zhuang, F.; Saint-Drenan, Y.-M.; Blanc, P. A New Approach for Satellite-Based Probabilistic Solar Forecasting with Cloud Motion Vectors. *Energies* **2021**, *14*, 4951. [CrossRef]
4. Rana, M.; Koprinska, I.; Agelidis, V.G. Univariate and multivariate methods for very short-term solar photovoltaic power forecasting. *Energy Convers. Manag.* **2016**, *121*, 380–390. [CrossRef]
5. Wang, H.; Yi, H.; Peng, J.; Wang, G.; Liu, Y.; Jiang, H.; Liu, W. Deterministic and probabilistic forecasting of photovoltaic power based on deep convolutional neural network. *Energy Convers. Manag.* **2017**, *153*, 409–422. [CrossRef]
6. De Giorgi, M.G.; Congedo, P.M.; Malvoni, M.; Laforgia, D. Error analysis of hybrid photovoltaic power forecasting models: A case study of mediterranean climate. *Energy Convers. Manag.* **2015**, *100*, 117–130. [CrossRef]
7. Alonso-Montesinos, J.; Batlles, F. Solar radiation forecasting in the short- and medium-term under all sky conditions. *Energy* **2015**, *83*, 387–393. [CrossRef]

8. Ruhang, X. The restriction research for urban area building integrated grid-connected PV power generation potential. *Energy* **2016**, *113*, 124–143. [CrossRef]
9. Voyant, C.; Notton, G.; Kalogirou, S.; Nivet, M.-L.; Paoli, C.; Motte, F.; Fouilloy, A. Machine learning methods for solar radiation forecasting: A review. *Renew. Energy* **2017**, *105*, 569–582. [CrossRef]
10. Yagli, G.M.; Yang, D.; Srinivasan, D. Automatic hourly solar forecasting using machine learning models. *Renew. Sustain. Energy Rev.* **2019**, *105*, 487–498. [CrossRef]
11. Mishra, M.; Nayak, J.; Naik, B.; Abraham, A. Deep learning in electrical utility industry: A comprehensive review of a decade of research. *Eng. Appl. Artif. Intell.* **2020**, *96*, 104000. [CrossRef]
12. Yu, Y.; Cao, J.; Zhu, J. An LSTM Short-Term Solar Irradiance Forecasting Under Complicated Weather Conditions. *IEEE Access* **2019**, *7*, 145651–145666. [CrossRef]
13. Yadav, A.P.; Kumar, A.; Behera, L. RNN Based Solar Radiation Forecasting Using Adaptive Learning Rate. In Proceedings of the Swarm, Evolutionary, and Memetic Computing, Chennai, India, 19–21 December 2013; Springer: Cham, Switzerland, 2013; pp. 442–452.
14. El Alani, O.; Abraim, M.; Ghennioui, H.; Ghennioui, A.; Ikenbi, I.; Dahr, F.E. Short term solar irradiance forecasting using sky images based on a hybrid CNN–MLP model. *Energy Rep.* **2021**, *7*, 888–900. [CrossRef]
15. Dairi, A.; Harrou, F.; Sun, Y.; Khadraoui, S. Short-Term Forecasting of Photovoltaic Solar Power Production Using Variational Auto-Encoder Driven Deep Learning Approach. *Appl. Sci.* **2020**, *10*, 8400. [CrossRef]
16. Huang, C.-J.; Kuo, P.-H. Multiple-Input Deep Convolutional Neural Network Model for Short-Term Photovoltaic Power Forecasting. *IEEE Access* **2019**, *7*, 74822–74834. [CrossRef]
17. Li, L.-L.; Cheng, P.; Lin, H.-C.; Dong, H. Short-term output power forecasting of photovoltaic systems based on the deep belief net. *Adv. Mech. Eng.* **2017**, *9*, 1687814017715983. [CrossRef]
18. Zhao, X.; Wei, H.; Wang, H.; Zhu, T.; Zhang, K. 3D-CNN-based feature extraction of ground-based cloud images for direct normal irradiance prediction. *Sol. Energy* **2019**, *181*, 510–518. [CrossRef]
19. Zhu, T.; Guo, Y.; Li, Z.; Wang, C. Solar Radiation Prediction Based on Convolution Neural Network and Long Short-Term Memory. *Energies* **2021**, *14*, 8498. [CrossRef]
20. Alharbi, F.R.; Csala, D. Wind Speed and Solar Irradiance Prediction Using a Bidirectional Long Short-Term Memory Model Based on Neural Networks. *Energies* **2021**, *14*, 6501. [CrossRef]
21. Abdel-Nasser, M.; Mahmoud, K. Accurate photovoltaic power forecasting models using deep LSTM-RNN. *Neural Comput. Appl.* **2019**, *31*, 2727–2740. [CrossRef]
22. Wen, L.; Zhou, K.; Yang, S.; Lu, X. Optimal load dispatch of community microgrid with deep learning based solar power and load forecasting. *Energy* **2019**, *171*, 1053–1065. [CrossRef]
23. Zang, H.; Cheng, L.; Ding, T.; Cheung, K.W.; Liang, Z.; Wei, Z.; Sun, G. Hybrid method for short-term photovoltaic power forecasting based on deep convolutional neural network. *IET Gener. Transm. Distrib.* **2018**, *12*, 4557–4567. [CrossRef]
24. Aprillia, H.; Yang, H.-T.; Huang, C.-M. Short-Term Photovoltaic Power Forecasting Using a Convolutional Neural Network–Salp Swarm Algorithm. *Energies* **2020**, *13*, 1879. [CrossRef]
25. Zhong, J.; Liu, L.; Sun, Q.; Wang, X. Prediction of Photovoltaic Power Generation Based on General Regression and Back Propagation Neural Network. *Energy Procedia* **2018**, *152*, 1224–1229. [CrossRef]
26. Lima, M.A.F.; Carvalho, P.C.; Fernández-Ramírez, L.M.; Braga, A.P. Improving solar forecasting using Deep Learning and Portfolio Theory integration. *Energy* **2020**, *195*, 117016. [CrossRef]
27. Jayalakshmi, N.; Shankar, R.; Subramaniam, U.; Baranilingesan, I.; Karthick, A.; Stalin, B.; Rahim, R.; Ghosh, A. Novel Multi-Time Scale Deep Learning Algorithm for Solar Irradiance Forecasting. *Energies* **2021**, *14*, 2404. [CrossRef]
28. Liebermann, S.; Um, J.-S.; Hwang, Y.; Schlüter, S. Performance Evaluation of Neural Network-Based Short-Term Solar Irradiation Forecasts. *Energies* **2021**, *14*, 3030. [CrossRef]
29. Krizhevsky, A.; Sutskever, I.; Hinton, G.E. ImageNet Classification with Deep Convolutional Neural Networks. 2012. Available online: https://proceedings.neurips.cc/paper/2012/hash/c399862d3b9d6b76c8436e924a68c45b-Abstract.html (accessed on 8 February 2022).
30. Yan, R.; Liao, J.; Yang, J.; Sun, W.; Nong, M.; Li, F. Multi-hour and multi-site air quality index forecasting in Beijing using CNN, LSTM, CNN-LSTM, and spatiotemporal clustering. *Expert Syst. Appl.* **2021**, *169*, 114513. [CrossRef]
31. Husein, M.; Chung, I.-Y. Day-Ahead Solar Irradiance Forecasting for Microgrids Using a Long Short-Term Memory Recurrent Neural Network: A Deep Learning Approach. *Energies* **2019**, *12*, 1856. [CrossRef]
32. Zhao, Z.; Chen, W.; Wu, X.; Chen, P.C.Y.; Liu, J. LSTM network: A deep learning approach for short-term traffic forecast. *IET Intell. Transp. Syst.* **2017**, *11*, 68–75. [CrossRef]
33. Barzegar, R.; Aalami, M.T.; Adamowski, J. Short-term water quality variable prediction using a hybrid CNN–LSTM deep learning model. *Stoch. Hydrol. Hydraul.* **2020**, *34*, 415–433. [CrossRef]
34. Gao, B.; Huang, X.; Shi, J.; Tai, Y.; Zhang, J. Hourly forecasting of solar irradiance based on CEEMDAN and multi-strategy CNN-LSTM neural networks. *Renew. Energy* **2020**, *162*, 1665–1683. [CrossRef]
35. Chen, Y.; Wang, Y.; Dong, Z.; Su, J.; Han, Z.; Zhou, D.; Zhao, Y.; Bao, Y. 2-D regional short-term wind speed forecast based on CNN-LSTM deep learning model. *Energy Convers. Manag.* **2021**, *244*, 114451. [CrossRef]

36. Tian, C.; Ma, J.; Zhang, C.; Zhan, P. A Deep Neural Network Model for Short-Term Load Forecast Based on Long Short-Term Memory Network and Convolutional Neural Network. *Energies* **2018**, *11*, 3493. [CrossRef]
37. Massaoudi, M.; S Refaat, S.; Abu-Rub, H.; Chihi, I.; Oueslati, F.S. PLS-CNN-BiLSTM: An end-to-end algorithm-based Savitzky–Golay smoothing and evolution strategy for load forecasting. *Energies* **2020**, *13*, 5464. [CrossRef]
38. Srivastava, N.; Hinton, G.; Krizhevsky, A.; Sutskever, I.; Salakhutdinov, R. Dropout: A simple way to prevent neural networks from overfitting. *J. Mach. Learn. Res.* **2014**, *15*, 1929–1958.
39. Montgomery, D.C.; Peck, E.A.; Vining, G.G. *Introduction to Linear Regression Analysis*; John Wiley & Sons: Hoboken, NJ, USA, 2021.
40. Awad, M.; Khanna, R. Support vector regression. In *Efficient Learning Machines*; Apress: Berkeley, CA, USA, 2015; pp. 67–80.
41. Maldonado, S.; González, A.; Crone, S. Automatic time series analysis for electric load forecasting via support vector regression. *Appl. Soft Comput.* **2019**, *83*, 105616. [CrossRef]
42. Najeebullah; Zameer, A.; Khan, A.; Javed, S.G. Machine Learning based short term wind power prediction using a hybrid learning model. *Comput. Electr. Eng.* **2015**, *45*, 122–133. [CrossRef]
43. Hong, Y.-Y.; Martinez, J.J.F.; Fajardo, A.C. Day-Ahead Solar Irradiation Forecasting Utilizing Gramian Angular Field and Convolutional Long Short-Term Memory. *IEEE Access* **2020**, *8*, 18741–18753. [CrossRef]
44. Li, G.; Xie, S.; Wang, B.; Xin, J.; Li, Y.; Du, S. Photovoltaic Power Forecasting with a Hybrid Deep Learning Approach. *IEEE Access* **2020**, *8*, 175871–175880. [CrossRef]
45. Kumar, D.; Mathur, H.D.; Bhanot, S.; Bansal, R.C. Forecasting of solar and wind power using LSTM RNN for load frequency control in isolated microgrid. *Int. J. Model. Simul.* **2021**, *41*, 311–323. [CrossRef]
46. Feng, C.; Zhang, J. SolarNet: A sky image-based deep convolutional neural network for intra-hour solar forecasting. *Sol. Energy* **2020**, *204*, 71–78. [CrossRef]
47. Zang, H.; Liu, L.; Sun, L.; Cheng, L.; Wei, Z.; Sun, G. Short-term global horizontal irradiance forecasting based on a hybrid CNN-LSTM model with spatiotemporal correlations. *Renew. Energy* **2020**, *160*, 26–41. [CrossRef]
48. Agga, A.; Abbou, A.; Labbadi, M.; El Houm, Y. Short-term self consumption PV plant power production forecasts based on hybrid CNN-LSTM, ConvLSTM models. *Renew. Energy* **2021**, *177*, 101–112. [CrossRef]
49. Kumari, P.; Toshniwal, D. Long short term memory–convolutional neural network based deep hybrid approach for solar irradiance forecasting. *Appl. Energy* **2021**, *295*, 117061. [CrossRef]
50. Singh, S. Noise impact on time-series forecasting using an intelligent pattern matching technique. *Pattern Recognit.* **1999**, *32*, 1389–1398. [CrossRef]
51. Sarp, S.; Kuzlu, M.; Cali, U.; Elma, O.; Guler, O. Analysis of False Data Injection Impact on AI-based Solar Photovoltaic Power Generation Forecasting. *arXiv* **2021**, arXiv:2110.09948. [CrossRef]